

RESPONSES TO  
NRC QUESTION  
ON THE  
DUANE ARNOLD ENERGY CENTER  
PUAR

PREPARED BY  
NUTECH ENGINEERS, INC.  
SAN JOSE, CALIFORNIA

PREPARED FOR  
IOWA ELECTRIC LIGHT AND POWER CO.

8409210193 840917  
PDR ADDCK 05000331  
P PDR

NRC QUESTION ON DUANE ARNOLD ENERGY CENTER

PIPING RESPONSE

ITEM 3a: Provide the theoretical background in support of Section 2 of the report, and describe how the Section 6 guidelines (i.e., cut-off frequency and equations 2.27 and 2.28) have been used in the analysis.

RESPONSE TO ITEM 3a:

- 1) The NUTECH computer program CMDOF utilized as the major building block, the Structural Mechanics Associates (SMA) developed program, CMDOF. This program was developed during the MK I Program for use by the Mark I Owners. The theoretical background for the coupling technology is contained in the SMA Report on CMDOF. The sections of this report covering the technical basis are included as Attachment A.
- 2) The computer program CMDOF was verified by SMA using several problems of differing complexity. Listed below are parameters for the four problems.

<u>EXAMPLE PROBLEM</u>	<u>NUMBER OF STRUCTURE</u>	<u>DOF's EQUIPMENT</u>	<u>NUMBER OF COUPLED DOF's</u>	<u>REMARKS</u>
1	5	4	3	Equipment attached to structure at 3 locations
2	5	2,3,4	4	3 separate equipment models attached to structure
3	12	9	3	3 coupled DOF's at 2 locations
4	1	1	1	Ungrounded equipment

As additional verification of the CMDOF program, an examination of the internal matrices of the coupling program was made by NUTECH. Chosen for examination was the "B-Delta" matrix. This matrix was selected since from it, the possibility for numerical instability, due to mass differences, can be readily determined. The numerical properties of the B-Delta matrix are discussed below, including a description of the physical meaning of the matrix. Three sample matrices are also included to illustrate these properties.

#### Physical Meaning of the B-Delta Matrix

For a decoupled torus analysis, it is assumed that the torus shell experiences some type of motion, while its decoupled "torus-attached" piping remains undisturbed. The compatibility between the torus and the attached piping is not considered. Equilibrium simply means zero internal reactions between the torus and the piping.

In reality however, the torus and the attached piping are coupled at the penetration point, which has some non-zero internal reactions. These reactions maintain the compatibility between the torus and the piping at the penetration point by eliminating the relative motions resulted from the assumed, decoupled torus analysis.

Thus, the coupling process at the penetration requires a dynamic flexibility matrix, which is the so-called B-Delta matrix in the CMDOF program. The coefficients of the matrix, by definition, are the relative (differential) accelerations between the decoupled torus and the decoupled "attached" piping due to unit and opposite (internal) reactions at the penetration. Using the matrix, we can then calculate the magnitude of internal reactions required to maintain compatibility.

#### Numerical Properties of the B-Delta Matrix

As a matrix of dynamic flexibility coefficients, the B-Delta matrix is, in matrix terminology, symmetric (due to the dynamic reciprocal law in structural mechanics) and positive definite (due to the stability of the torus and attached piping).

For torus attached piping applications, the diagonal terms of the matrix are quite uniform in magnitude. In order to illustrate this, three typical piping systems analyzed with CMDOF were reviewed and their "B-Delta" matrices extracted. These three matrices were chosen to represent the range of piping systems analyzed in the MK1 program. Figure 1 is the matrix for a 2" turbine drain line. This was typically the smallest line analyzed using full coupling techniques. Figure 2 contains the matrix for an 8" pressure relief line and figure 3 contains the matrix for a 24" RHR suction line, the largest piping analyzed.

It can be seen that the diagonal terms of the three sample matrices are within 4-5 orders of magnitude (maximum 1-13,500). The large digital computers with 60 bits per word and 15 digits of accuracy used for CMDOF analysis will not suffer numerical problems with this range. This is especially true for the B-Delta matrix found in a torus-attached piping application where the matrix size, i.e., the number of coupling degrees of freedom, is small and far less than typically large structural stiffness matrices.

3) The CMDOF computer program was utilized for large bore torus attached piping analysis. In certain cases the coupling analysis was utilized for small bore lines (2" diameter).

The use of coupling techniques for small bore piping was infrequent as the benefits of coupling were quite small. Conversely, coupling for large bore piping exhibited significant coupling benefits.

To illustrate the effect of pipe size on coupling, four typical piping systems were examined and the coupled and uncoupled time histories plotted together. These time histories include both the smallest (2") and larger (20") systems analyzed. Listed below are the figure numbers and the corresponding line size.

Figure 4-8	2" diameter
9-13	4" diameter
14-18	6" diameter
19-21	20" diameter

These plots confirm the expected variation of coupling benefit with pipe size.

ATTACHMENT A

## 2. TECHNICAL BASIS

### 2.1 ASSUMPTIONS

1. At the attachment point, the structure uncoupled and coupled acceleration time histories and the equipment reaction time history for all degrees-of-freedom are assumed to vary linearly between time steps. This assumption is common to many dynamic analysis programs and the time step size for this coupling program does not have to be any smaller than for most other dynamic analysis programs. A time step equal to  $(0.1/f)$  where  $f$  is the highest natural frequency of interest is generally considered adequate.
2. Both the structure and the attached equipment are considered to behave linearly elastic. Superposition is used extensively in this program.
3. Sufficient structural and equipment modes are included to accurately model the structure and equipment at the degree-of-freedom (dof) of interest.

### 2.2 COMPATIBILITY AND SUPERPOSITION

Figure 2-1 illustrates an uncoupled structure model and uncoupled equipment models which are attached to the structure at a series of different nodes with one dof (dof) of coupling per node. Another model which would be just as valid for use in conjunction with the theory which follows is one in which the equipment is attached to the structure at only a couple of nodes but there are multiple degrees of coupling at each attachment node. In the following discussion, there are assumed to be NC coupled dof between the structure and equipment.

As shown in Figure 2-1, the uncoupled structure is subjected to an input force loading  $F(t_i)$  which in the absence of the attached equipment results in a series of uncoupled accelerations  $a_{U_j}(t_i)$  for each attachment mode at time  $t_i$ . By knowing the modal characteristics of the uncoupled structure and uncoupled equipment models (frequency, eigenvector, participation factor for each of the NC attachment dof) the coupling reaction  $R_j(t_i)$  for each dof applied by the equipment on the structure at time  $t_i$  can be determined from the coupled accelerations  $a_{C_j}$  defined at all previous time steps  $t_0$  through  $t_{i-1}$ . This reaction  $R_j(t_i)$  on the uncoupled structure model results in the structural response acceleration  $a_{R_j}(t_i)$  at dof  $j$  where  $a_{R_j}(t_i)$  is the acceleration at time  $t_i$  due to the equipment reaction  $R_j$  for all previous times considering the contributions of all NC attachment dof between the equipment and structure. By using superposition, the coupled acceleration of the attachment point for dof  $j$  is given by:

$$a_{C_j}(t_i) = a_{U_j}(t_i) + a_{R_j}(t_i) \quad (2.1)$$

Note that  $a_{R_j}(t_i)$  is due to the equipment reaction time histories  $R_k$  for all coupling DOF through time  $t_i$  which, in turn, are due to the coupled acceleration time histories  $a_{C_j}$  for all coupled DOF through time  $t_i$ .

Compatibility requires that the coupled accelerations  $a_{C_j}(t_i)$  and the reactions  $R_j(t_i)$  at the attachment points be identical for the structure and attached equipment for every time point  $t_i$ . Similarly, superposition requires that Equation 2.1 be satisfied

at every point  $t_i$ . At the outset, only the uncoupled response time histories defined by  $a_{U_j}(t_i)$  are known at each time point  $t_i$ . The essence of this program is to determine the reaction  $R_j(t_i)$  and reaction acceleration  $a_{R_j}(t_i)$  for all NC attachment dof time point by time point so that compatibility and superposition are satisfied at every time point  $t_i$ .

### 2.3 STRUCTURE RESPONSE DUE TO EQUIPMENT REACTIONS

The reaction acceleration  $a_{R_k}(t_i)$  for the structure at the equipment attachment node for dof k can be defined in terms of the reaction forces  $R_j(t_i)$  by:

$$a_{R_k}(t_i) = \sum_{j=1}^{NC} \sum_{m=1}^{M_S} PF_{S_{j,m}} \cdot \phi_{S_{k,m}} \cdot \ddot{Y}_{j,m}(t_i) \quad (2.2)$$

where NC represents the total number of coupling degrees-of-freedom considered,  $M_S$  represents the total number of important structure modes,  $PF_{S_{j,m}}$  is the uncoupled structure participation factor for mode m associated with an applied unit force/moment at dof j, and  $\phi_{S_{k,m}}$  is the structural eigenvector for attachment dof k, for uncoupled structure mode m. The uncoupled structure m-th mode acceleration due to reaction  $R_j(t_i)$  at dof j and time  $t_i$  is given by:

$$\ddot{Y}_{j,m}(t_i) + 2\lambda_{S_m} \omega_{S_m} \dot{Y}_{j,m}(t_i) + \omega_{S_m}^2 Y_{j,m}(t_i) = -R_j(t_i) \quad (2.3)$$

where  $\lambda_{S_m}$  is the modal structural damping ratio and  $\omega_{S_m}$  is the modal angular natural frequency for uncoupled structure mode m.

Given the response at time  $t_{i-1}$ , the modal response at time  $t_i$  for the attachment node, dof  $j$ , can be determined using the Nigam-Jennings technique (Reference 1) as follows:

$$\left. \begin{aligned}
 Y_{j,m}(t_i) &= Y_{j,m}^*(t_i) + B_{12S_m} \cdot \Delta R_j(t_i) \\
 Y_{j,m}^*(t_i) &= A_{11S_m} \cdot Y_{j,m}(t_{i-1}) + A_{12S_m} \cdot \dot{Y}_{j,m}(t_{i-1}) + B_{11S_m} \cdot R_j(t_{i-1}) \\
 \dot{Y}_{j,m}(t_i) &= \dot{Y}_{j,m}^*(t_i) + B_{22S_m} \cdot \Delta R_j(t_i) \\
 \dot{Y}_{j,m}^*(t_i) &= A_{21S_m} \cdot Y_{j,m}(t_{i-1}) + A_{22S_m} \cdot \dot{Y}_{j,m}(t_{i-1}) + B_{21S_m} \cdot R_j(t_{i-1})
 \end{aligned} \right\} (2.4)$$

By substituting Equation 2.4 into Equation 2.3,

$$\left. \begin{aligned}
 \ddot{Y}_{j,m}(t_i) &= \ddot{Y}_{j,m}^*(t_i) - \Delta R_j(t_i) \cdot \left[ 1 + 2 \lambda_{S_m} \omega_{S_m} B_{22S_m} + \omega_{S_m}^2 B_{12S_m} \right] \\
 \ddot{Y}_{j,m}^*(t_i) &= -R_j(t_{i-1}) - 2\lambda_{S_m} \omega_{S_m} \dot{Y}_{j,m}^*(t_i) - \omega_{S_m}^2 Y_{j,m}^*(t_i)
 \end{aligned} \right\} (2.5)$$

where  $R_j(t_{i-1})$  represents the equipment reaction for attachment dof  $j$  at the previous time point  $t_{i-1}$ , and  $\Delta R_j(t_i)$  represents the change in reaction for attachment dof  $j$  during the time interval from  $t_{i-1}$  to  $t_i$ . The change in reaction  $\Delta R_j(t_i)$  is unknown because the equipment solution has not been completed through time  $t_i$ . However, the reaction  $R_j(t_{i-1})$  for the previous time point is known so that the quantities  $Y_{j,m}^*(t_i)$ ,  $\dot{Y}_{j,m}^*(t_i)$ ,  $\ddot{Y}_{j,m}^*(t_i)$  can be evaluated for all the attachment dof for each structure mode  $m$  at time  $t_i$ . Using  $\ddot{Y}_{j,m}^*(t_i)$  the reaction acceleration  $a_{R_k}(t_i)$  at dof  $k$  for all NC dof can be determined using Equation 2.2 as follows:

$$\ddot{a}_{R_k}^*(t_i) = \sum_{j=1}^{NC} \sum_{m=1}^{M_S} PF_{S_{j,m}} \cdot \phi_{S_{k,m}} \cdot \ddot{Y}_{j,m}^*(t_i) \quad (2.6)$$

The reaction acceleration  $a_{R_k}^*(t_i)$  represents the reaction acceleration for the attachment node, dof k, that would result if no change in reactions occurred between time  $t_{i-1}$  and  $t_i$  (i.e.,  $\Delta R_j(t_i) = 0$ ).

The change in reaction acceleration for dof k,  $a_{\Delta R_k}(t_i)$  due to the change in reaction  $\Delta R_j(t_i)$  as obtained from Equations 2.2 and 2.5 is:

$$a_{\Delta R_k}(t_i) = \sum_{j=1}^{NC} A_{\Delta S_{k,j}} \cdot \Delta R_j(t_i) \quad (2.7)$$

where:

$$A_{\Delta S_{k,j}} = - \sum_{m=1}^{M_S} PF_{S_{j,m}} \cdot \phi_{S_{k,m}} \left[ 1 + 2\lambda_{S_m} \omega_{S_m} B_{22S_m} + \omega_{S_m}^2 B_{12S_m} \right] \quad (2.8)$$

The quantity  $A_{\Delta S_{k,j}}$  represents the change in the structure reaction acceleration at dof k, due to a unit change in the reaction/moment at attachment dof j during the time step and is independent of the structural response or time step. This quantity simply depends upon the uncoupled structure modal properties and the time step size  $\Delta t$ .

The total reaction acceleration for attachment dof k at time  $t_i$  is given by:

$$a_{R_k}(t_i) = a_{R_k}^*(t_i) + a_{\Delta R_k}(t_i) \quad (2.9)$$

The coupled acceleration for attachment dof K as obtained from Equation 2.1 is thus:

$$a_{c_k}(t_i) = a_{cs_k}^*(t_i) + a_{\Delta R_k}(t_i) \quad (2.10)$$

where:

$$a_{cs_k}^*(t_i) = a_{u_k}(t_i) + a_{R_k}^*(t_i) \quad (2.11)$$

The Nigam-Jennings coefficients used in Equations 2.4 and 2.5 for calculating the modal structural response are derived from the coefficients in Reference 1 and are as follows:

$$\begin{aligned}
A_{11} &= \omega^2 B_{11} + 1 \\
A_{12} &= -B_{21} \\
A_{21} &= \omega^2 B_{21} \\
A_{22} &= A_{11} + 2\lambda\omega B_{21} \\
B_{11} &= \Delta t_i B_{22} \\
B_{12} &= -e^{-\lambda\omega\Delta t_i} \left[ \frac{(2\lambda^2-1)}{\omega^3\Delta t_i} \frac{\sin \omega_D \Delta t_i}{\omega_D} + \frac{2\lambda}{\omega^3\Delta t_i} \cos \omega_D \Delta t_i \right] - \frac{1}{\omega^2} + \frac{2\lambda}{\omega^3\Delta t_i} \\
B_{21} &= -e^{-\lambda\omega\Delta t_i} \left[ \frac{\sin \omega_D \Delta t_i}{\omega_D} \right] \\
B_{22} &= e^{-\lambda\omega\Delta t_i} \left[ \frac{\cos \omega_D \Delta t_i}{\omega^2 \Delta t_i} + \left( \frac{\lambda}{\omega\Delta t_i} \right) \frac{\sin \omega_D \Delta t_i}{\omega_D} \right] - \frac{1}{\omega^2\Delta t_i}
\end{aligned} \tag{2.12}$$

where the damped modal natural frequency  $\omega_D$  is given by

$$\omega_D = \omega\sqrt{1-\lambda^2} \tag{2.13}$$

Note that all of the coefficients are defined in terms of  $B_{12}$ ,  $B_{21}$ , and  $B_{22}$ . Further note that when the product  $\omega\Delta t_i$  is small, both  $B_{12}$  and  $B_{22}$  are obtained by the subtraction of two nearly equal numbers. On a computer with seven to eight significant figure accuracy it has been found that the coefficients  $B_{12}$ , and  $B_{22}$  can be evaluated both faster and more accurately using a series expansion in lieu of Equation 2.12 whenever

$$\omega\Delta t_i < 0.3$$

The series expansion used is

$$\begin{aligned}
B_{12} &= -e^{-\lambda\omega\Delta t_i} \left( \frac{\Delta t_i^2}{6} \right) \left[ 1 + \frac{\lambda\omega\Delta t_i}{2} + \frac{(4\lambda^2-1)}{20} (\omega\Delta t_i)^2 + \frac{\lambda(3\lambda^2-1)}{60} (\omega\Delta t_i)^3 + \frac{(1-5\lambda^2+9\lambda^4)}{840} (\omega\Delta t_i)^4 \right] \\
B_{22} &= -e^{-\lambda\omega\Delta t_i} \left( \frac{\Delta t_i}{2} \right) \left[ 1 + \frac{\lambda\omega\Delta t_i}{3} + \frac{(2\lambda^2-1)(\omega\Delta t_i)^2}{12} + \frac{\lambda(2\lambda^2-1)(\omega\Delta t_i)^3}{60} + \frac{(1-3\lambda^2+3\lambda^4)(\omega\Delta t_i)^4}{360} \right]
\end{aligned} \tag{2.14}$$

## 2.4

UNCOUPLED EQUIPMENT RESPONSE TO ATTACHMENT POINT REACTION

Using a development similar to that shown for the structure in Section 2.3, the following definitions are possible. The reaction acceleration  $a_{ce_k}(t_i)$  for dof k at the corresponding equipment attachment node is identical to the coupled acceleration  $a_{c_k}(t_i)$ . Thus, the coupled acceleration at dof k can be defined in terms of the coupling reaction forces  $R_j(t_i)$  by:

$$a_{c_k}(t_i) = -\sum_{j=1}^{NC} \sum_{m=1}^{M_E} PF_{E_{j,m}} \cdot \phi_{E_{k,m}} \cdot \ddot{Z}_{j,m}(t_i) \quad (2.15)$$

where NC represents the total number of degrees-of-freedom considered at the equipment attachment nodes,  $M_E$  represents the total number of important equipment modes,  $PF_{E_{j,m}}$  is the uncoupled equipment participation factor for mode m associated with an applied unit force/moment at attachment dof j, and  $\phi_{E_{k,m}}$  is the equipment eigenvector for attachment dof k for uncoupled equipment mode m. The uncoupled equipment m-th mode acceleration for an applied reaction  $R_j(t_i)$  at dof j and time  $t_i$  is given by:

$$\ddot{Z}_{j,m}(t_i) + 2\lambda_{E_m} \omega_{E_m} \dot{Z}_{j,m}(t_i) + \omega_{E_m}^2 Z_{j,m}(t_i) = -R_j(t_i) \quad (2.16)$$

where  $\lambda_{E_m}$  is the modal equipment damping ratio and  $\omega_{E_m}$  is the modal angular natural frequency for uncoupled equipment mode m.

A set of equations identical to Equations 2.4 and 2.5 may be written for the equipment by making the following substitutions. All letters  $Y, \dot{Y}, \ddot{Y}, Y^*, \dot{Y}^*,$  and  $\ddot{Y}^*$  must be replaced by  $Z, \dot{Z}, \ddot{Z}, Z^*, \dot{Z}^*,$  and  $\ddot{Z}^*$  respectively while keeping all subscripts the same. All Nigam-Jennings coefficients for the structure  $A_{11S}, A_{12S}, \dots, B_{22S}$  must be replaced by the analogous equipment Nigam-Jennings response coefficients  $A_{11E}, A_{12E}, \dots, B_{22E}$ . Interpretation of the resulting equations for the equipment modal accelerations, velocities, and displacements, are similar to those given in Section 2.3 for the uncoupled structure.

Since the quantity  $R_j(t_{i-1})$  for the previous time point is known, the quantities  $Z_{j,m}^*(t_i), \dot{Z}_{j,m}^*(t_i), \ddot{Z}_{j,m}^*(t_i)$  can be evaluated for all NC attachment dof for each equipment mode  $m$  at time  $t_i$ . Using  $\ddot{Z}_{j,m}^*(t_i)$ , the reaction acceleration  $a_{ce_k}^*(t_i)$  can be determined from Equation 2.15 as follows:

$$a_{ce_k}^*(t_i) = - \sum_{j=1}^{NC} \sum_{m=1}^{M_E} PF_{E_{j,m}} \cdot \phi_{E_{k,m}} \cdot \ddot{Z}_{j,m}^*(t_i) \quad (2.17)$$

The reaction acceleration  $a_{ce_k}^*(t_i)$  represents the reaction acceleration for the equipment attachment node, dof  $k$ , that would result if no change in reactions occurred between time  $t_{i-1}$  and  $t_i$ .

The change in the reaction acceleration for dof  $k$ ,  $a_{\Delta c_k}(t_i)$  due to the change in reaction  $\Delta R_j(t_i)$  is:

$$a_{\Delta c_k}(t_i) = \sum_{j=1}^{NC} A_{\Delta E_{k,j}} \cdot \Delta R_j(t_i) \quad (2.18)$$

where

$$A_{\Delta E_{k,j}} = \sum_{m=1}^{M_E} PF_{E_{j,m}} \cdot \phi_{E_{k,m}} \left[ 1 + 2\lambda_{E_m} \omega_{E_m} B_{22E_m} + \omega_{E_m}^2 B_{12E_m} \right] \quad (2.19)$$

The quantity  $A_{\Delta E_{k,j}}$  represents the change in the equipment reaction acceleration at dof k due to a unit change in reaction/moment at attachment dof j during the time step.

The coupled acceleration for dof k is equal to:

$$a_{C_k}(t_i) = a_{ce_k}^*(t_i) + a_{\Delta C_k}(t_i) \quad (2.20)$$

In order to find the quantities  $a_{\Delta R_k}(t_i)$  for the structure (Equation 2.7) and  $a_{\Delta C_k}(t_i)$  for the equipment (Equation 2.18) for all NC attachment dof, the change in the coupling reactions  $\Delta R_j(t_i)$  must be found for all dof at time step  $t_i$ . This may be done by setting Equation 2.10 equal to Equation 2.20 and solving for  $\Delta R_j(t_i)$ . Thus, for time step  $t_i$ :

$$[B_{\Delta}] \{ \Delta R \} = \{ C \} \quad (2.21)$$

where:

$$\{ \Delta R \} = [B_{\Delta}]^{-1} \{ C \} \quad (2.22)$$

$$B_{\Delta_{k,j}} = A_{\Delta S_{k,j}} - A_{\Delta E_{k,j}} \quad (2.23)$$

$$C_k(t_i) = a_{ce_k}^*(t_i) - a_{cs_k}^*(t_i) \quad (2.24)$$

By Maxwell's Law the displacement of dof k due to a unit force at dof j must equal the displacement at dof j due to a unit force of dof k, therefore the  $[B_{\Delta}]$  matrix must be symmetric. Thus:

$$B_{\Delta k,j} = B_{\Delta j,k} \quad (2.24a)$$

Lack of symmetry is an indication that improper eigenvector values or improper participation factors have been input to the coupling program.

Thus, the change in reaction for each dof j,  $\Delta R_j(t_i)$  during the time step are determined from all of the dof accelerations  $C_k(t_i)$  corresponding to the difference in the structure and equipment accelerations resulting from no change in the reactions during the time step  $t_i$  and the matrix  $[B_{\Delta}]^{-1}$  which is a constant and is independent of the time history analysis.

Once the change in the coupling reactions  $\Delta R_j(t_i)$  are known for all NC attachment dof, the coupled acceleration for each attachment dof may be calculated for time step  $t_i$  by Equations 2.7 and 2.10. The total coupling reactions for time step  $t_i$ , dof j, are then given by:

$$R_j(t_i) = R_j(t_{i-1}) + \Delta R_j(t_i) \quad (2.25)$$

Thus, it is possible to calculate the coupled structural response at time step  $t_i$  using the results of the previous time step  $t_{i-1}$ . Once the coupled response is known for all NC attachment dof for time step  $t_i$ , the analysis can proceed to the next time point  $t_{i+1}$  and continue the correction of the uncoupled acceleration time history by marching time point by time point.

1.4

NOTATION

$A_{11E_m}, \dots, B_{22E_m}$  = Nigam-Jennings coefficients for equipment mode m.

$A_{11S_m}, \dots, B_{22S_m}$  = Nigam-Jennings coefficients for uncoupled structure mode m.

$a_{c_j}(t_i)$  = Coupled acceleration of structure attachment point degree-of-freedom j at time  $t_i$ .

$a_{R_j}(t_i)$  = Reaction acceleration of structure attachment point degree-of-freedom j at time  $t_i$ .

$a_{u_j}(t_i)$  = Uncoupled acceleration of structure attachment point degree-of-freedom j at time  $t_i$ .

- $d_{c_j}(t_i)$  = Coupled displacement of structure attachment point degree-of-freedom  $j$  at time  $t_i$ .
- $d_{u_j}(t_i)$  = Uncoupled displacement of structure attachment point degree-of-freedom  $j$  at time  $t_i$ .
- $f_{E_m}$  = Equipment mode frequency (Hz) for mode  $m$ .
- $f_{S_m}$  = Equipment mode frequency (Hz) for mode  $m$ .
- $j, k$  = Attachment point degree-of-freedom numbers.
- $m$  = Mode number.
- $M_E$  = Total number of equipment modes.
- $M_S$  = Total number of structure modes.
- $NC$  = Total number of degrees-of-freedom at which coupling is considered between structure and equipment.
- $PF_{E_{j,m}}$  = Uncoupled equipment participation factor for mode  $m$  associated with an applied unit force/moment at attachment degree-of-freedom  $j$  for the equipment attachment node.

- $PF_{S_{j,m}}$  = Uncoupled structure participation factor for mode  $m$  associated with applied unit force/moment at attachment degree-of-freedom  $j$  for the equipment attachment node on the structure.
- $R_j(t_i)$  = Coupling reaction acceleration at time  $t_i$  for degree-of-freedom  $j$ .
- $\Delta R_j(t_i)$  = Change in coupling reaction acceleration from time  $t_{i-1}$  to time  $t_i$  at degree-of-freedom  $j$
- $t_i$  = Time at time step  $i$ .
- $V_{C_j}(t_i)$  = Coupled velocity of structure attachment point degree-of-freedom  $j$  at time  $t_i$ .
- $\ddot{Y}_{m,j}(t_i), \dot{Y}_{m,j}(t_i), Y_{m,j}(t_i)$  = Modal acceleration, velocity, and displacement for uncoupled structure mode  $m$ , dof  $j$  at time  $t_i$ , respectively.
- $\ddot{Z}_{m,j}(t_i), \dot{Z}_{m,j}(t_i), Z_{m,j}(t_i)$  = Modal relative acceleration, velocity, and displacement for uncoupled equipment mode  $m$ , dof  $j$  at time  $t_i$ , respectively.

$\Delta t_i$  = Time step size from time  $t_{i-1}$  to time  $t_i$ .

$\lambda_{E_m}$  = Ratio of m-th equipment mode damping to critical damping.

$\lambda_{S_m}$  = Ratio of m-th structure mode damping to critical damping.

$\phi_{E_{j,m}}$  = Uncoupled equipment eigenvector for degree-of-freedom j and mode m.

$\phi_{S_{j,m}}$  = Uncoupled structure eigenvector value for degree-of-freedom j and mode m.

$\omega_{E_m}$  = Circular natural frequency for equipment mode m.

$\omega_{S_m}$  = Circular natural frequency for structure mode m.

1	-12.39				
2	-.1609	14.13	(symmetric)		
3	1.827	-2.504	16.19		
4	.0402	.0727	.2508	.1029	
5	-.5180	.0286	-.1699	-.0037	.1093
DOF	1	2	3	4	5

Figure 1  
 B-Delta Matrix from a 2" HPCI Turbine Drain

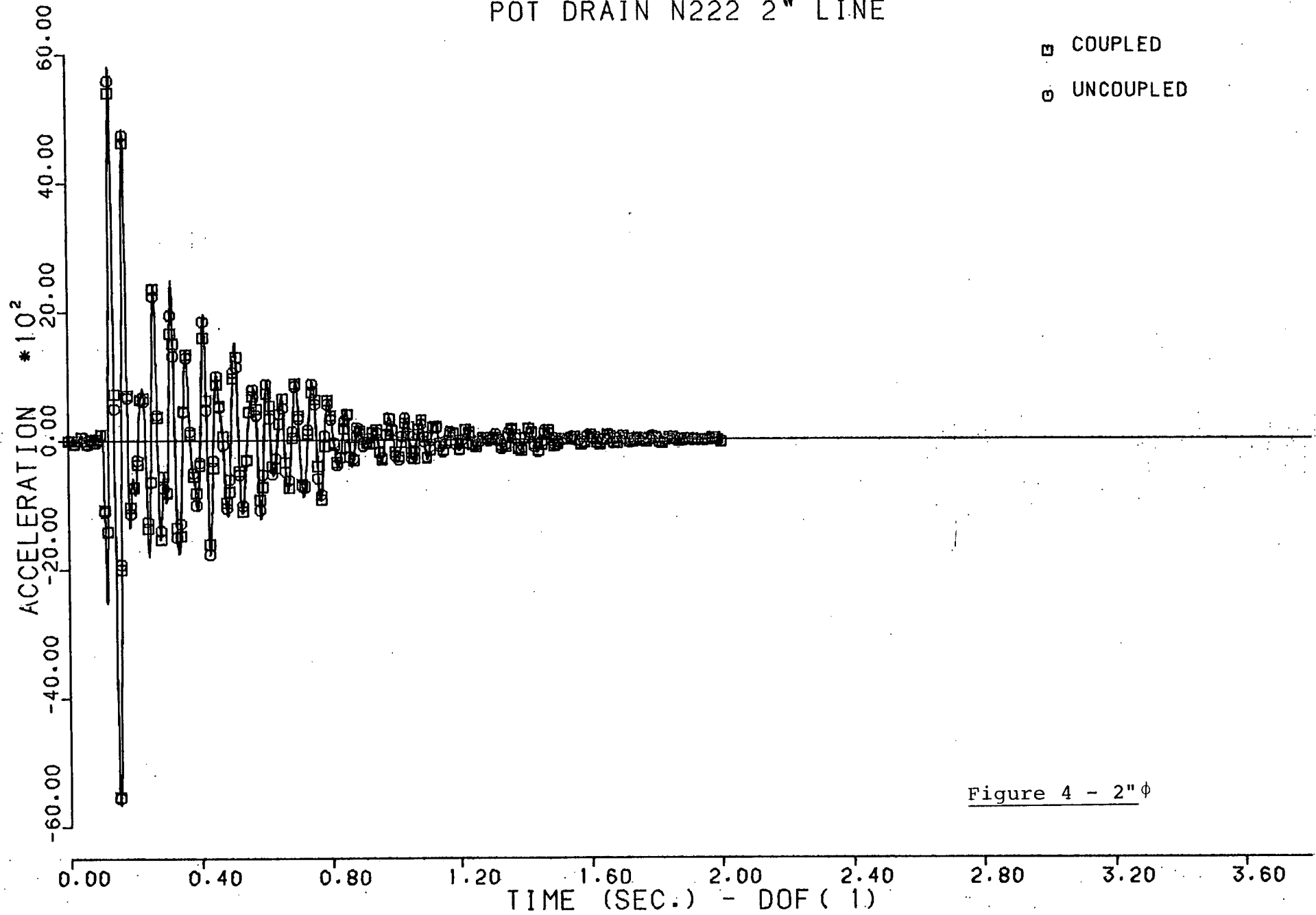
1	2	3	4	5	6	7	8	9	10	11	12	13	14	15	DOF
-44.14	-7.588	-28.86	1.722	-9.853	.0217	.0026	-.0529	.0002	.0003	.0521	.0208	.1072	-.0056	-.0227	1
	-65.85	7.726	14.87	-1.733	-.0047	-.0025	.0096	-.0007	.0001	-.0273	.0155	-.0331	-.0052	.0050	2
		-24.07	-1.784	-6.703	-.0272	-.0096	-.0475	-.0009	-.0020	-.1008	-.0251	-.1479	.0016	.0235	3
			-4.074	.4701	.0017	.0147	.0064	.0013	.0004	.0062	-.0054	.0101	-.0007	.0016	4
				-2.704	.0177	.0017	.0112	.0004	-.0018	-.0109	-.0008	.0003	.0016	-.0038	5
					-1.287	.0568	-.0706	-.0061	.0360	-.0668	-.0168	-.0983	-.0011	.0049	6
						-.7525	-.1716	.0021	.0063	.0212	.0027	.0352	.0134	.0002	7
							-1.669	-.0150	-.0047	-.1535	-.0330	-.2943	.0010	.0099	8
								-.0049	-.0006	-.0020	-.0016	-.0016	.0006	.0002	9
						(symmetric)			-.0059	.0024	.0007	.0028	.00004	-.0012	10
										-44.83	7.403	27.95	-1.734	-9.851	11
											+65.94	7.512	14.87	1.736	12
												-25.29	-1.809	6.696	13
													-4.077	-.4722	14
														-2.707	15

Figure 2  
B-Delta Matrix from an 8" RHR Pressure Relief

1	-10.97				
2	-.4010	-8.188	(symmetric)		
3	-.0525	.6121	-1.131		
4	1.061	-.3145	-.6404	-376.9	
5	115.6	-13.57	3.123	33.63	6080.
DOF	1	2	3	4	5

Figure 3  
 B-Delta Matrix from a 24" RHR Suction

POT DRAIN N222 2" LINE



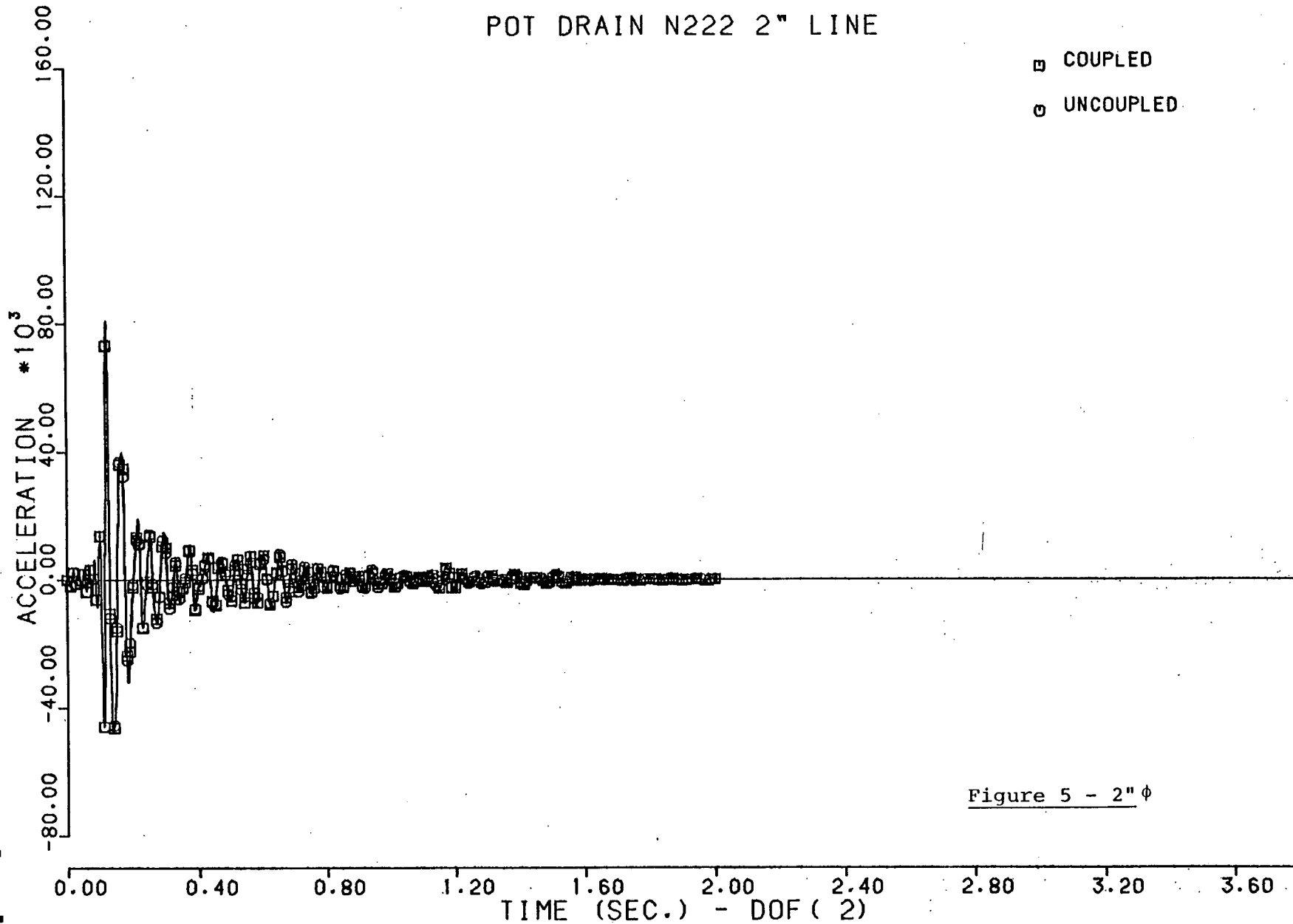


Figure 5 - 2"  $\phi$

POT DRAIN N222 2" LINE

- ▣ COUPLED
- UNCOUPLED

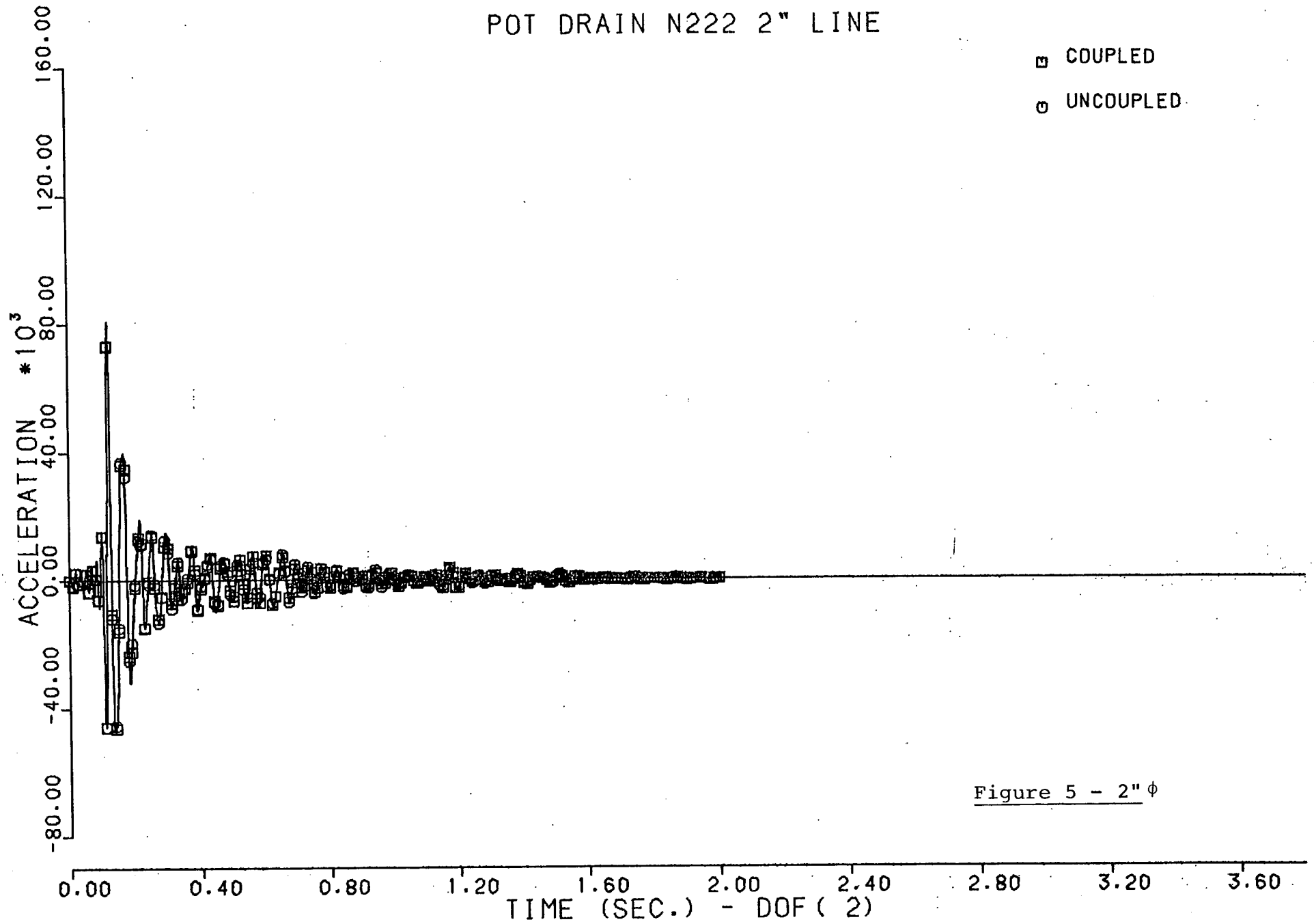


Figure 5 - 2"  $\phi$

POT DRAIN N222 2" LINE

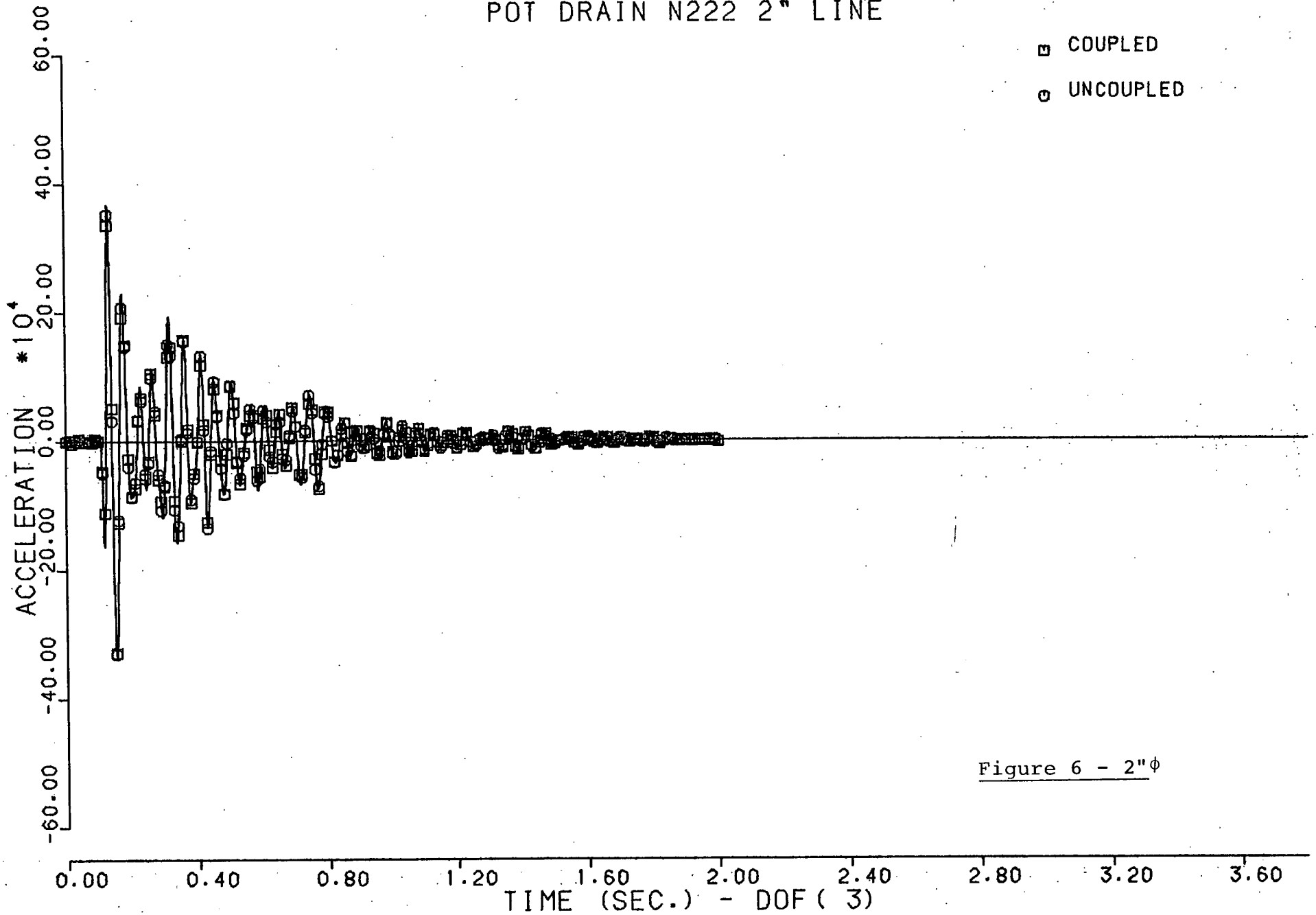


Figure 6 - 2"φ

POT DRAIN N222 2" LINE

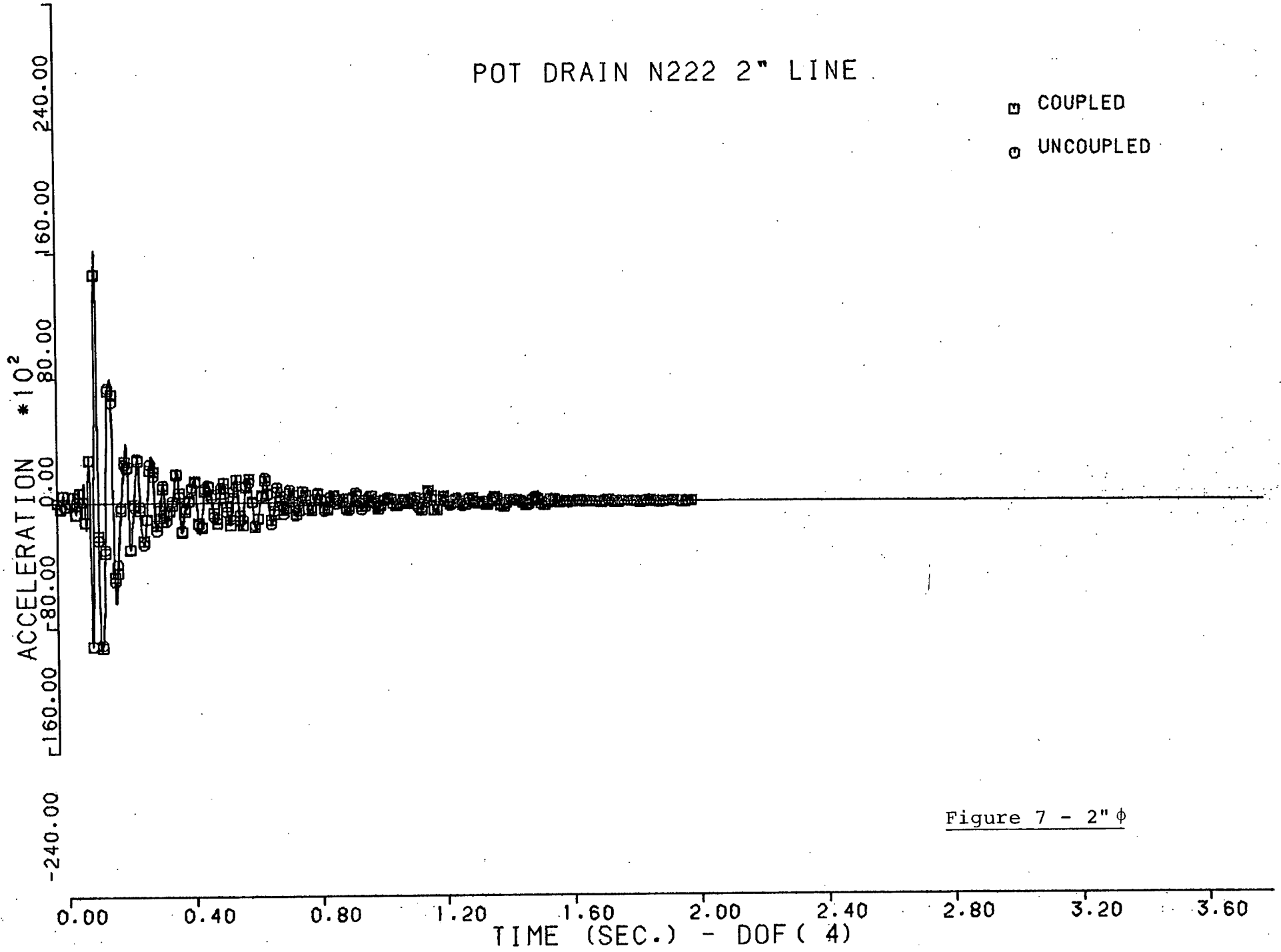


Figure 7 - 2"  $\phi$

POT DRAIN N222 2" LINE

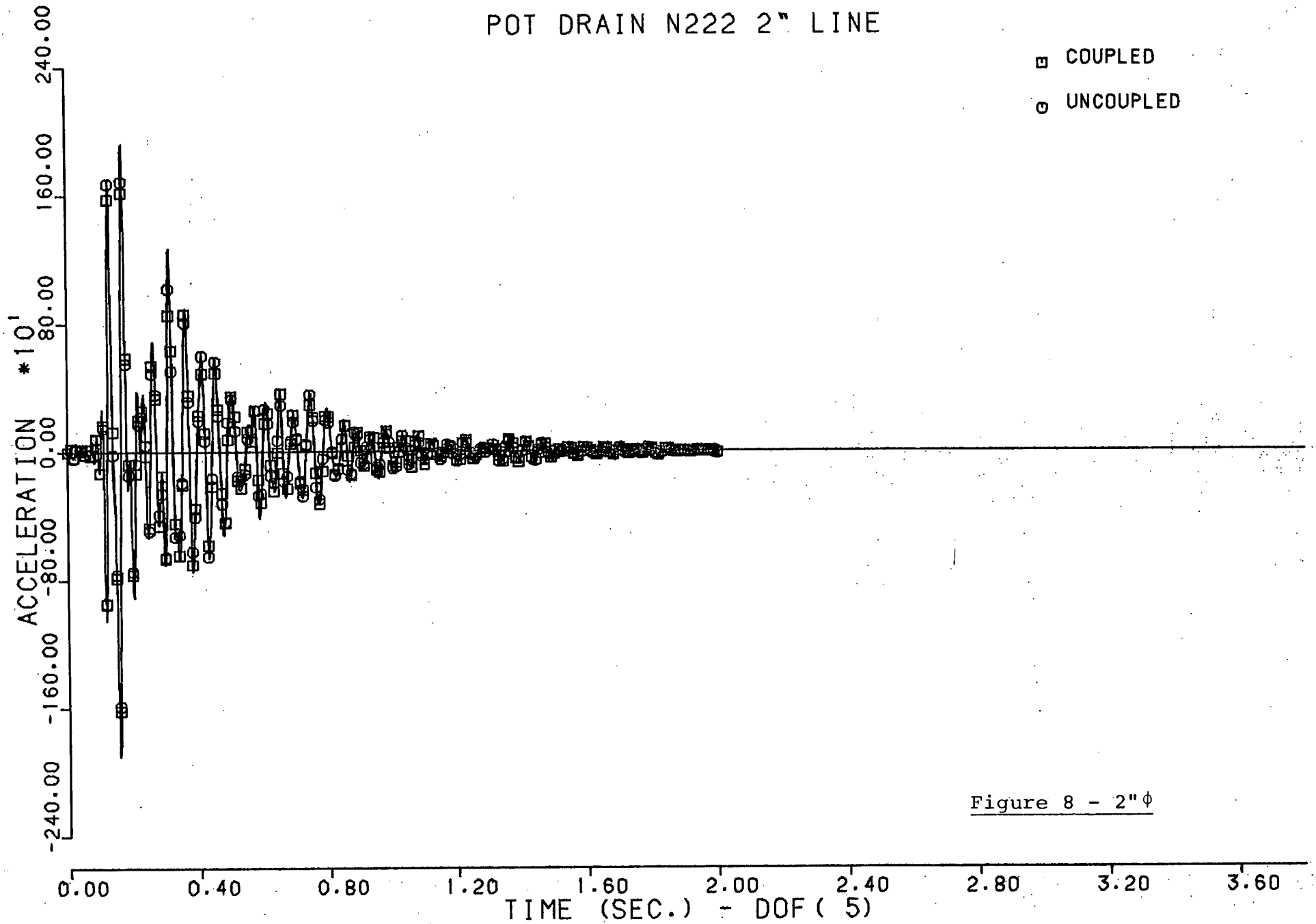
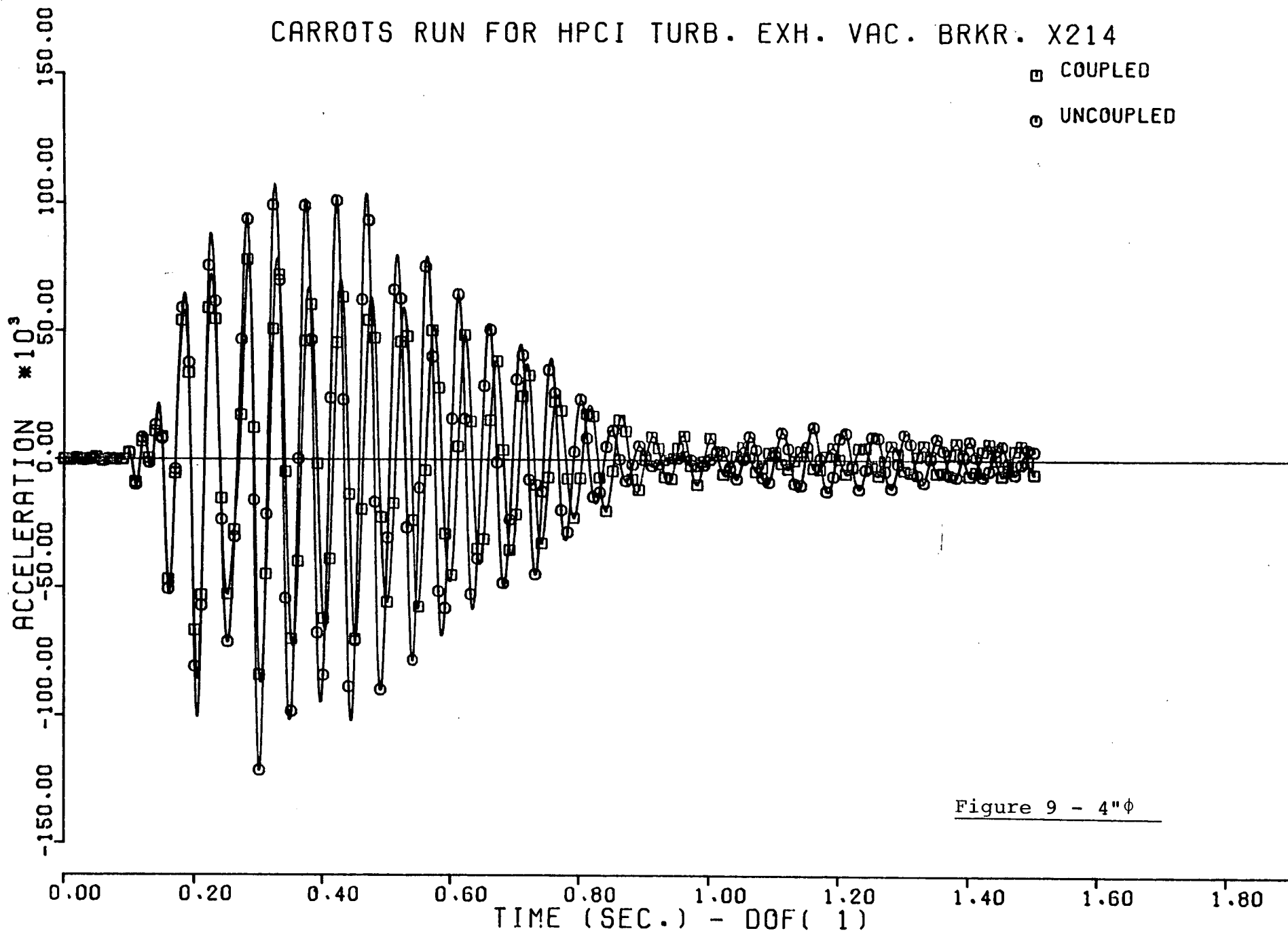
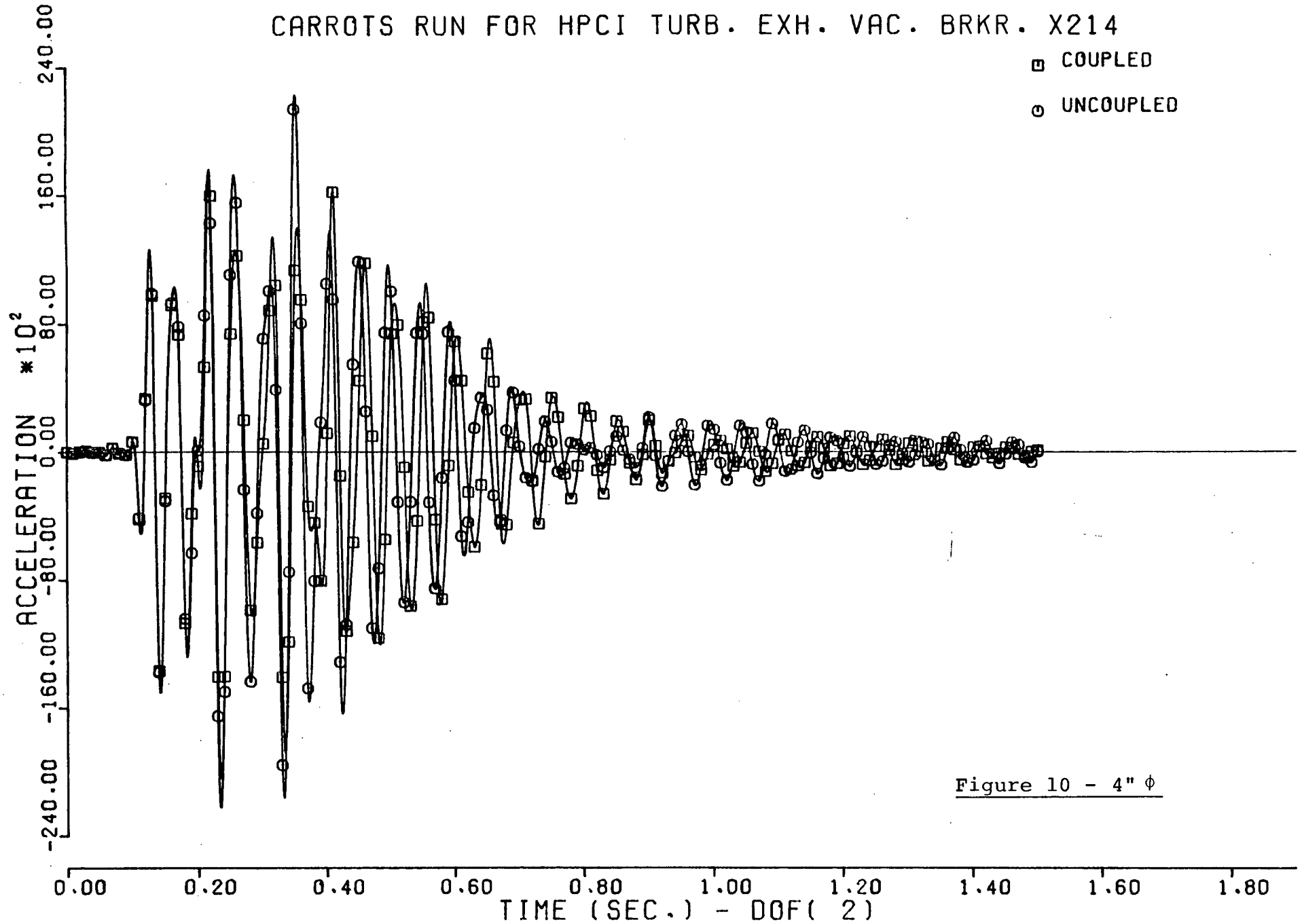


Figure 8 - 2"  $\phi$

CARROTS RUN FOR HPCI TURB. EXH. VAC. BRKR. X214



CARROTS RUN FOR HPCI TURB. EXH. VAC. BRKR. X214



CARROTS RUN FOR HPCI TURB. EXH. VAC. BRKR. X214

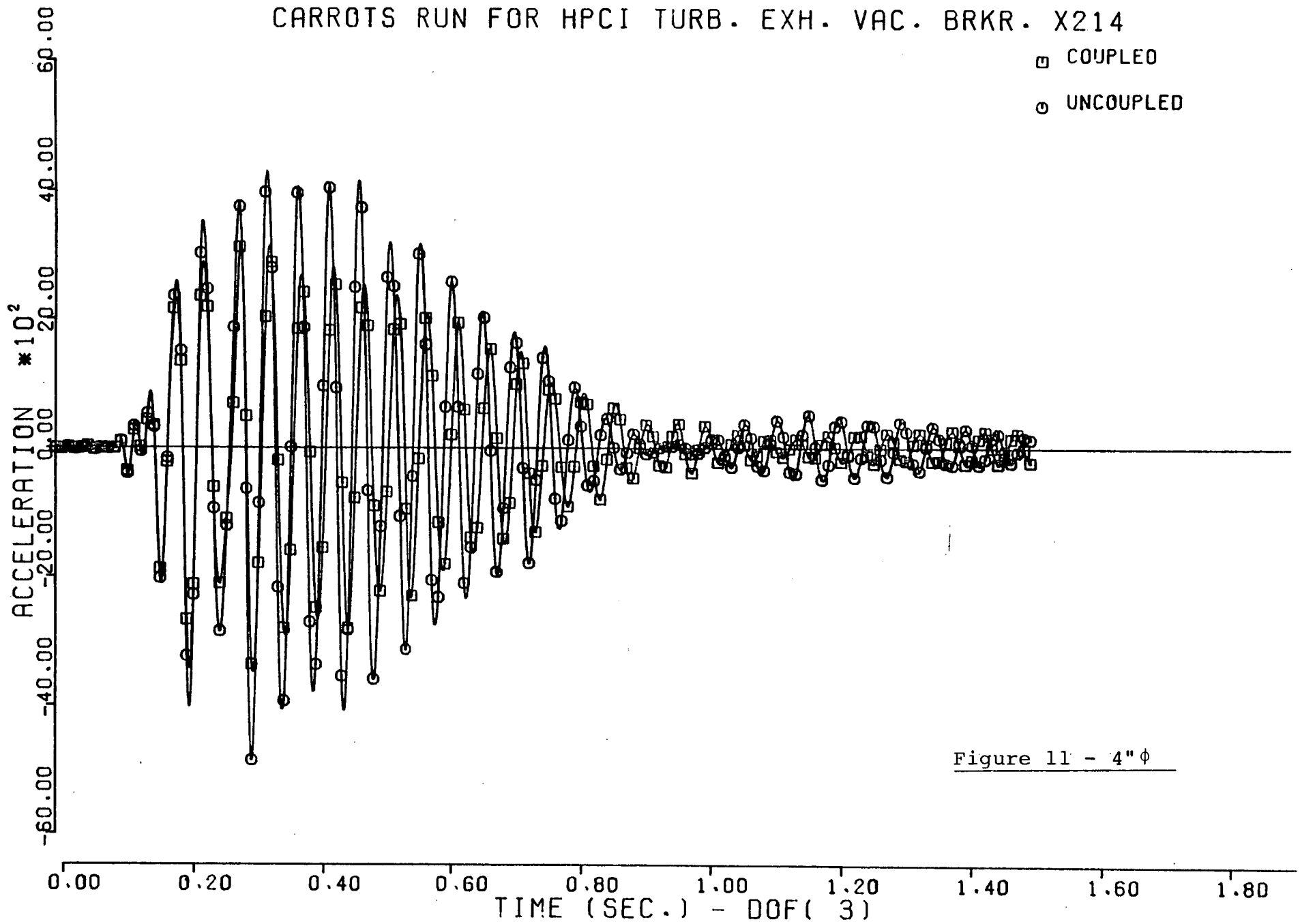


Figure 11 - 4"φ

CARROTS RUN FOR HPCI TURB. EXH. VAC. BRKR. X214

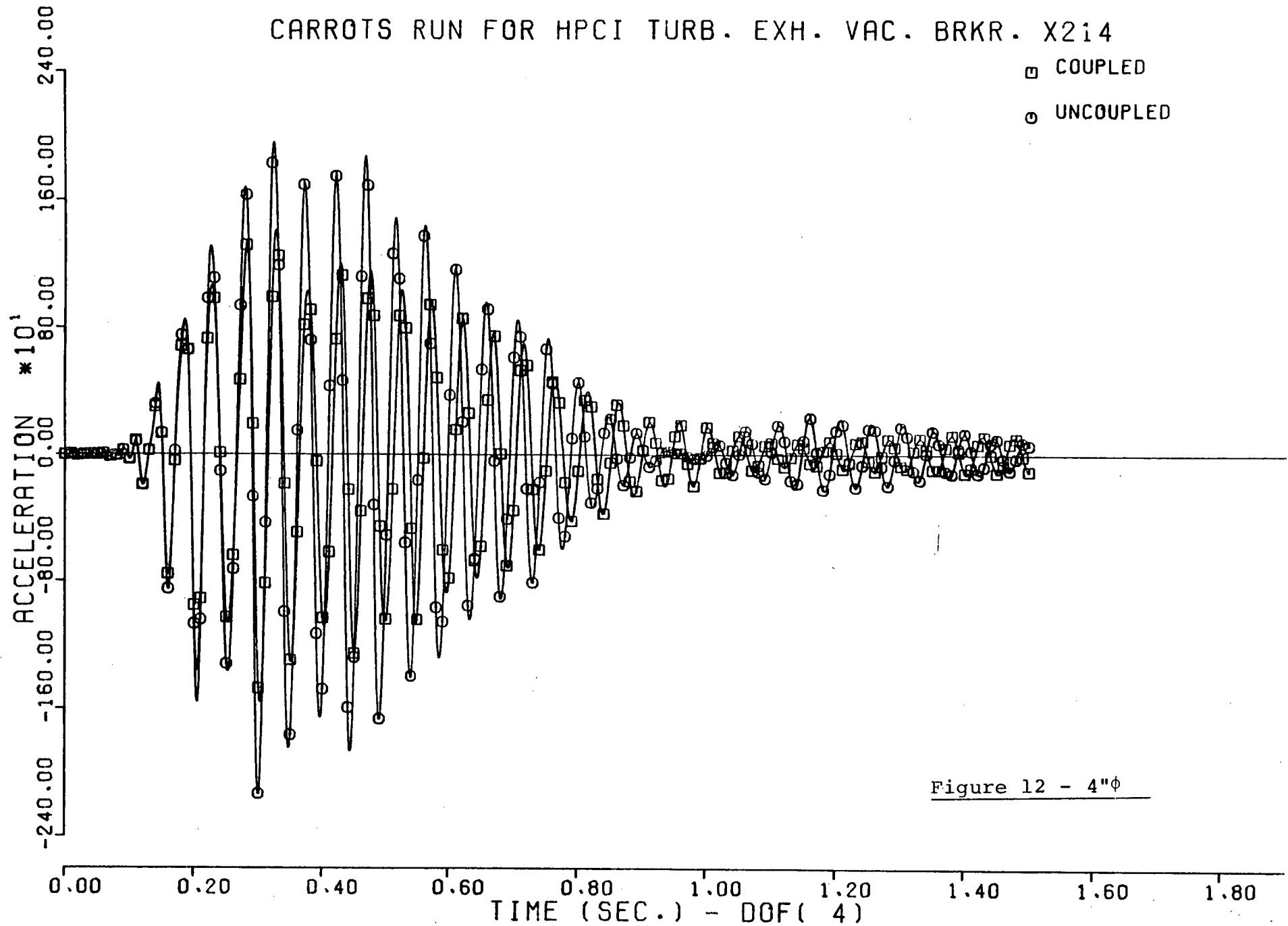
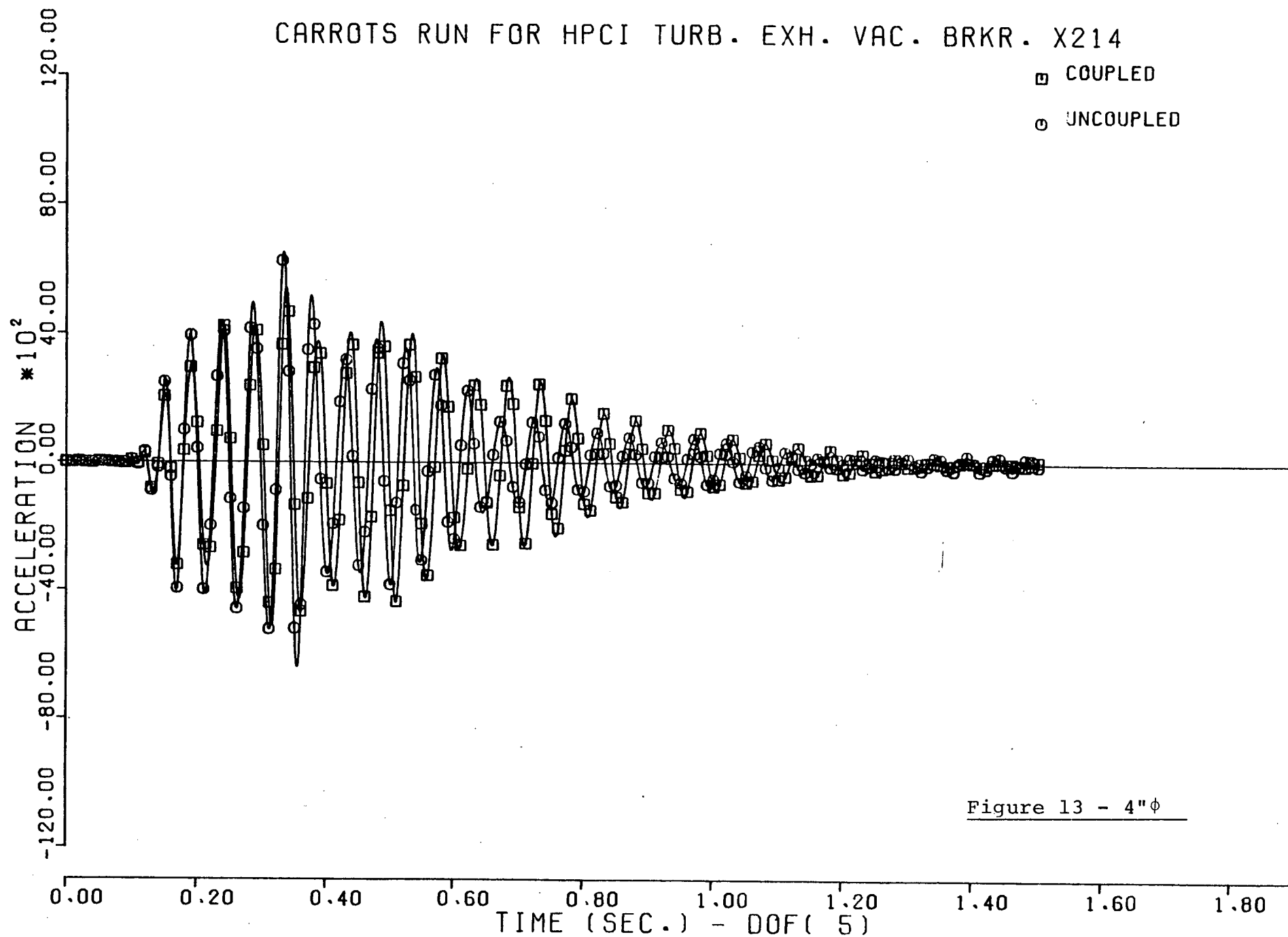


Figure 12 - 4"φ

CARROTS RUN FOR HPCI TURB. EXH. VAC. BRKR. X214



CPS-18  
RUN-3C  
SRV-2

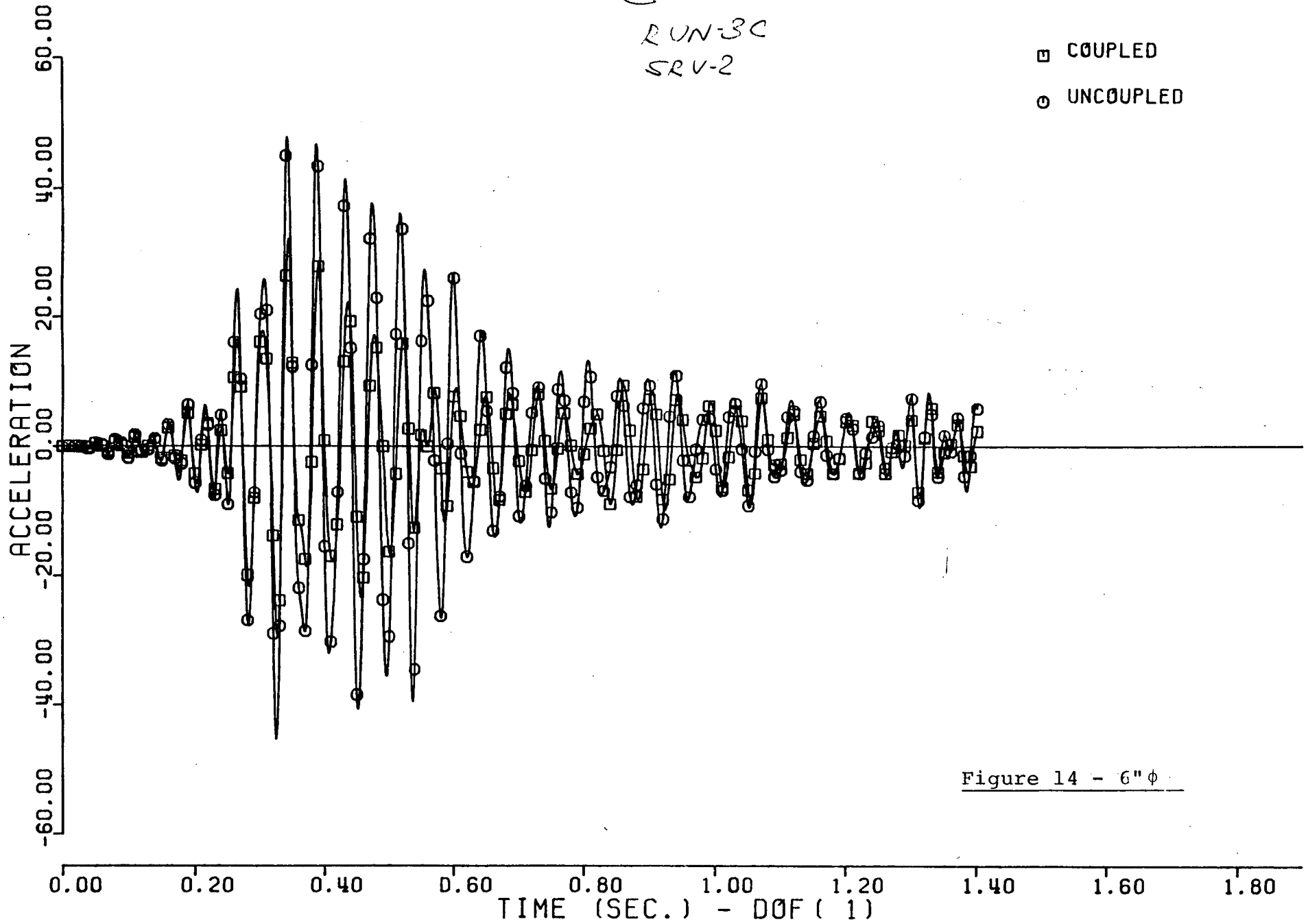


Figure 14 - 6"φ

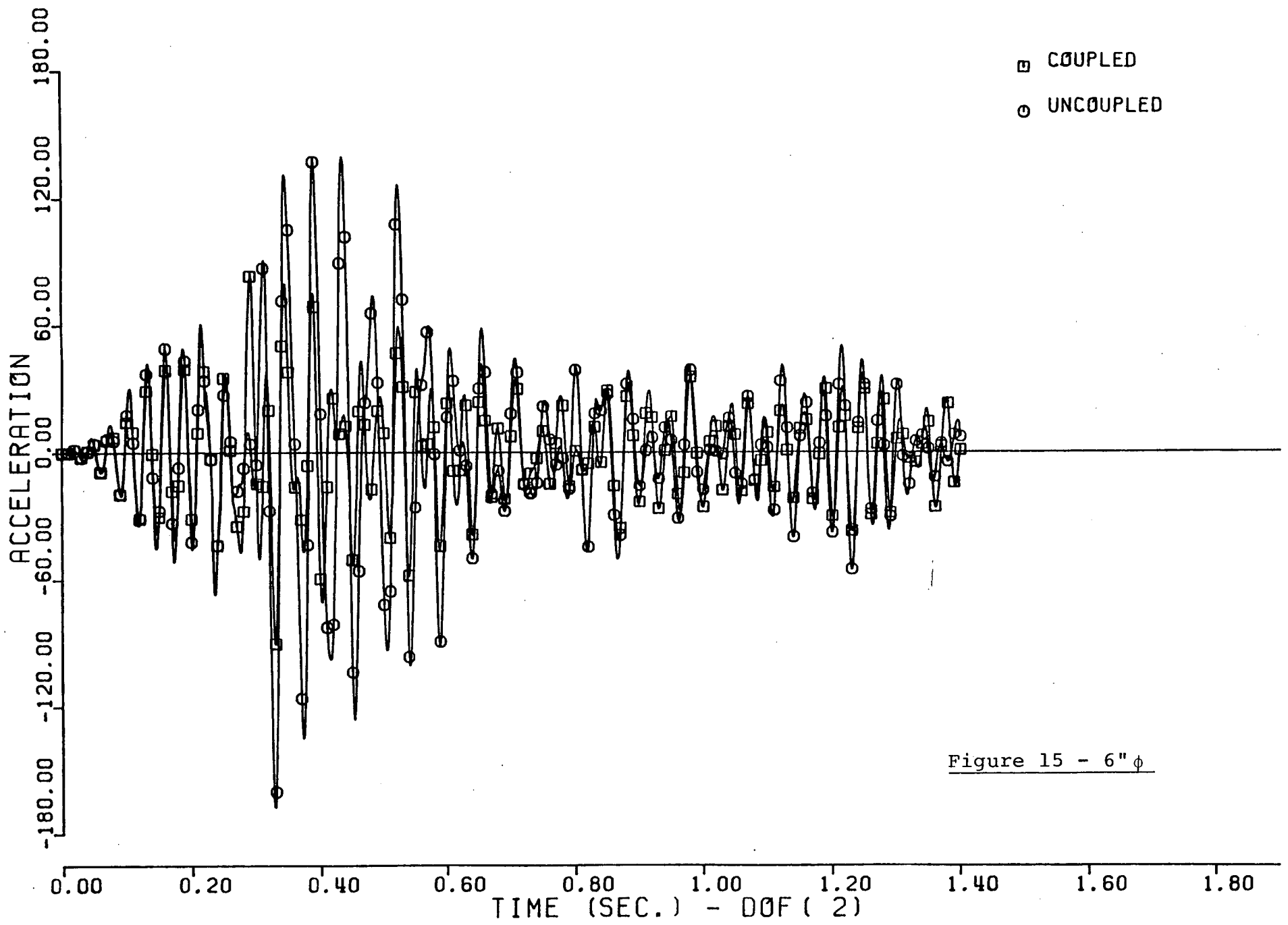


Figure 15 - 6"  $\phi$

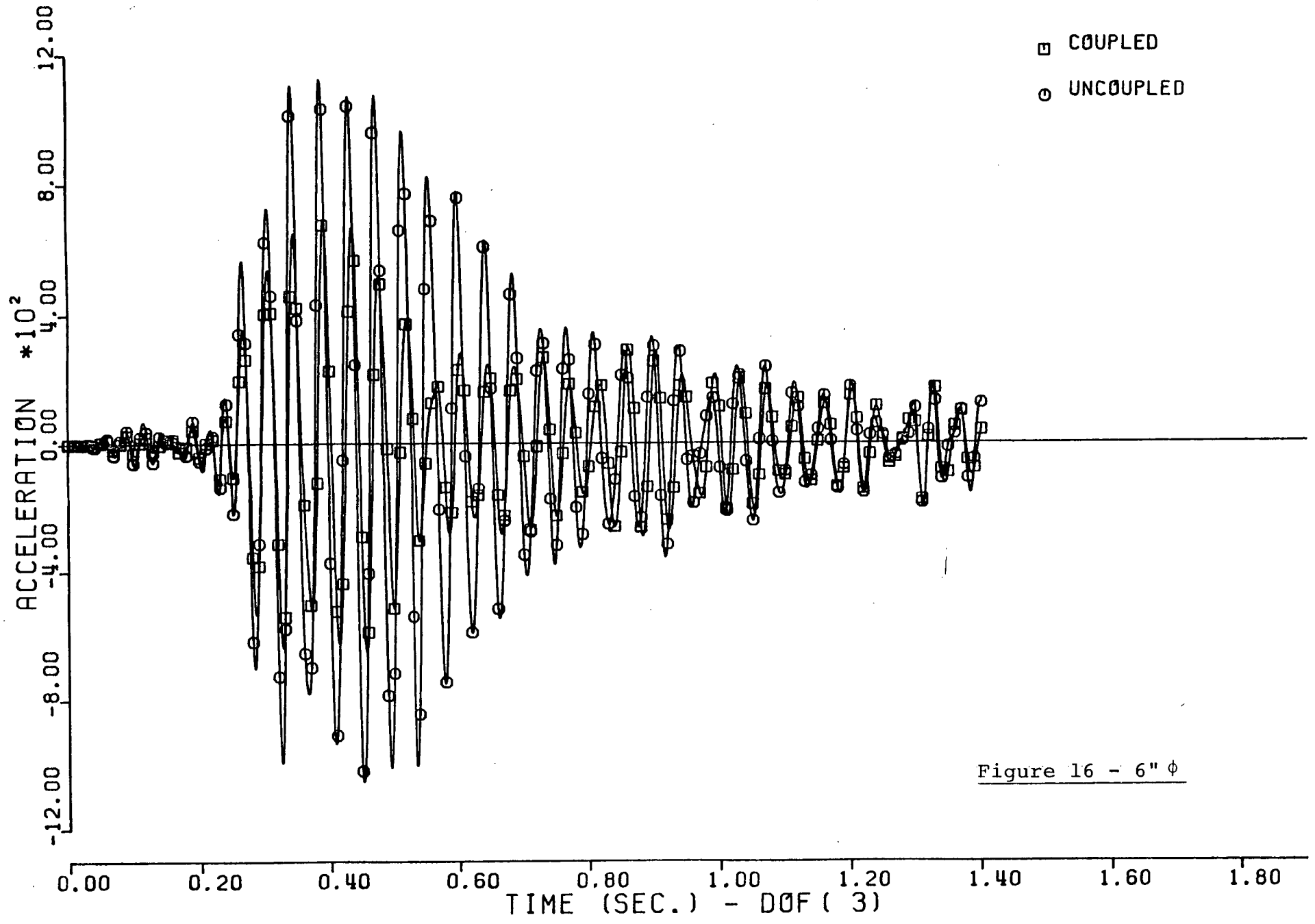


Figure 16 - 6"  $\phi$

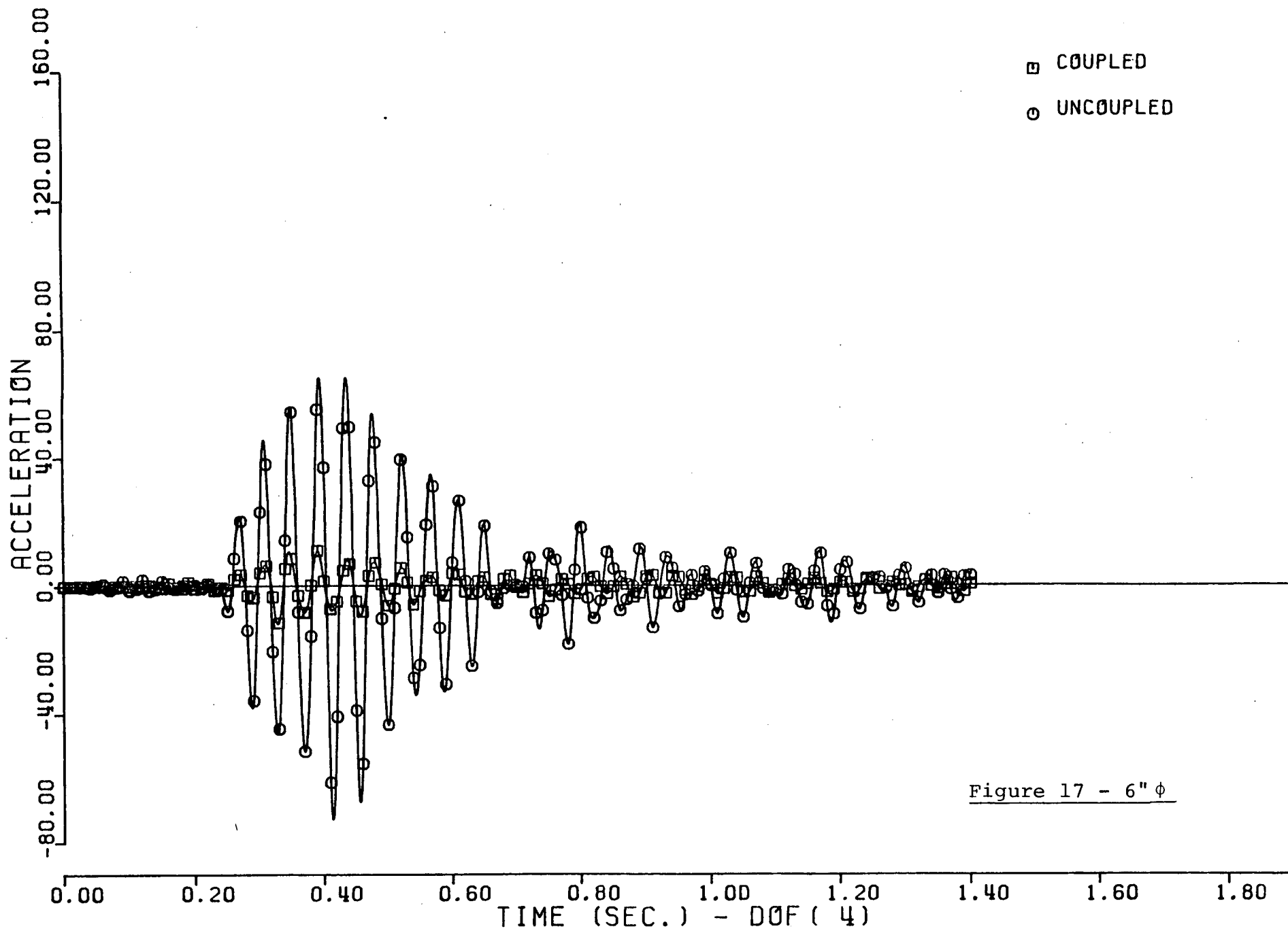


Figure 17 - 6"  $\phi$

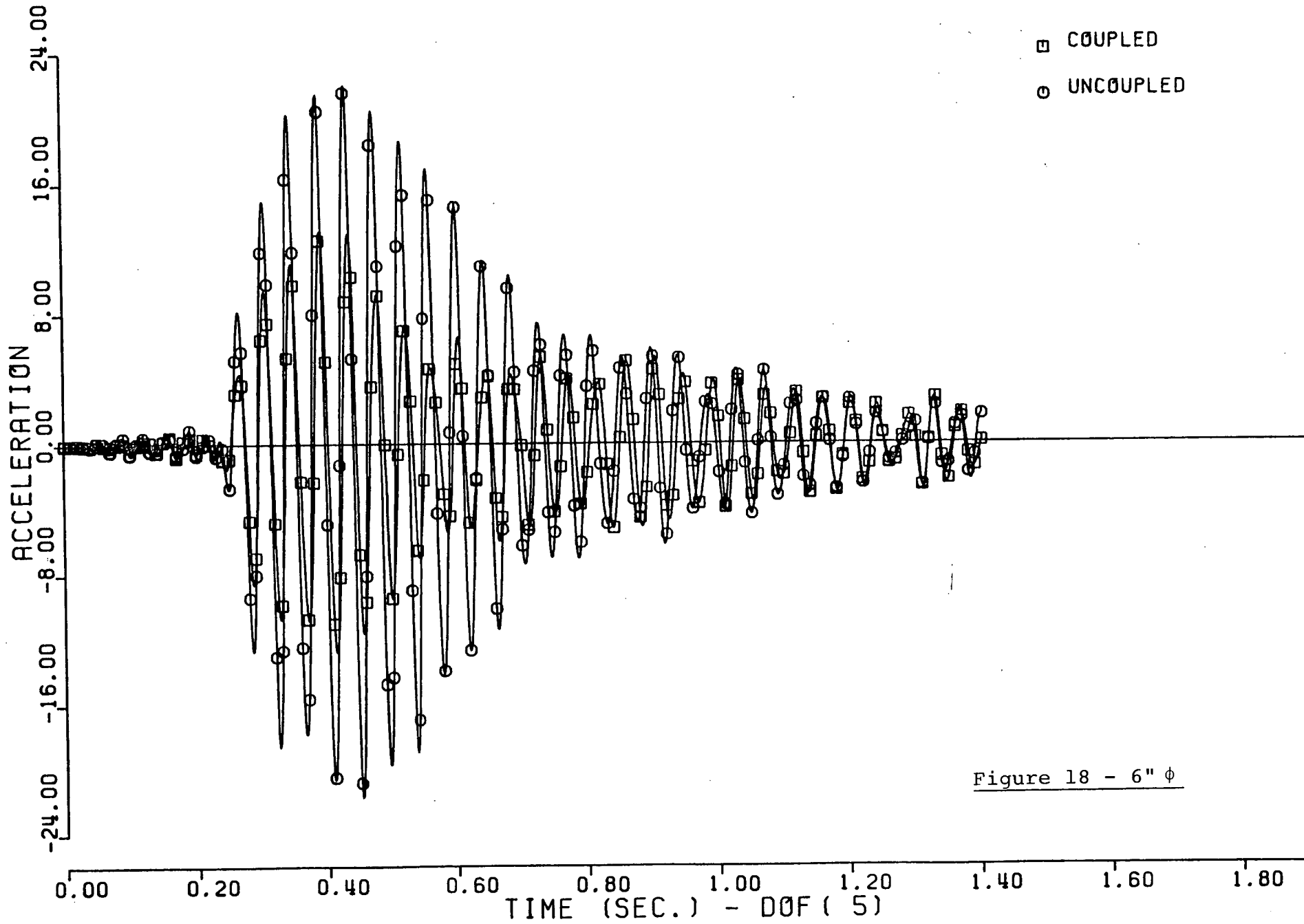


Figure 18 - 6"  $\phi$

CORE SPRAY PUMP SUCTION SOUTH X224A

6.18

- COUPLED
- UNCOUPLED

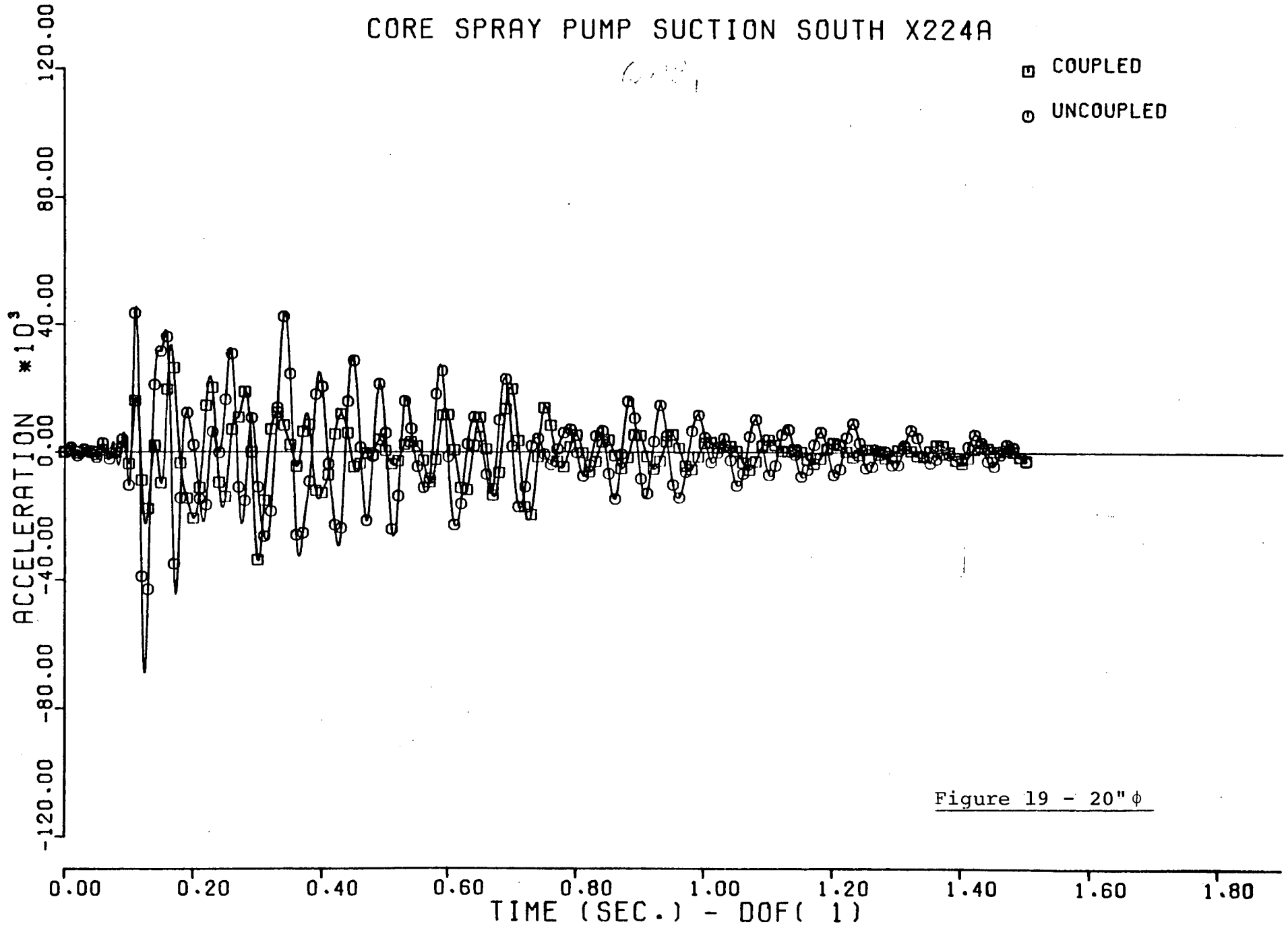


Figure 19 - 20" φ

CORE SPRAY PUMP SUCTION SOUTH X224A

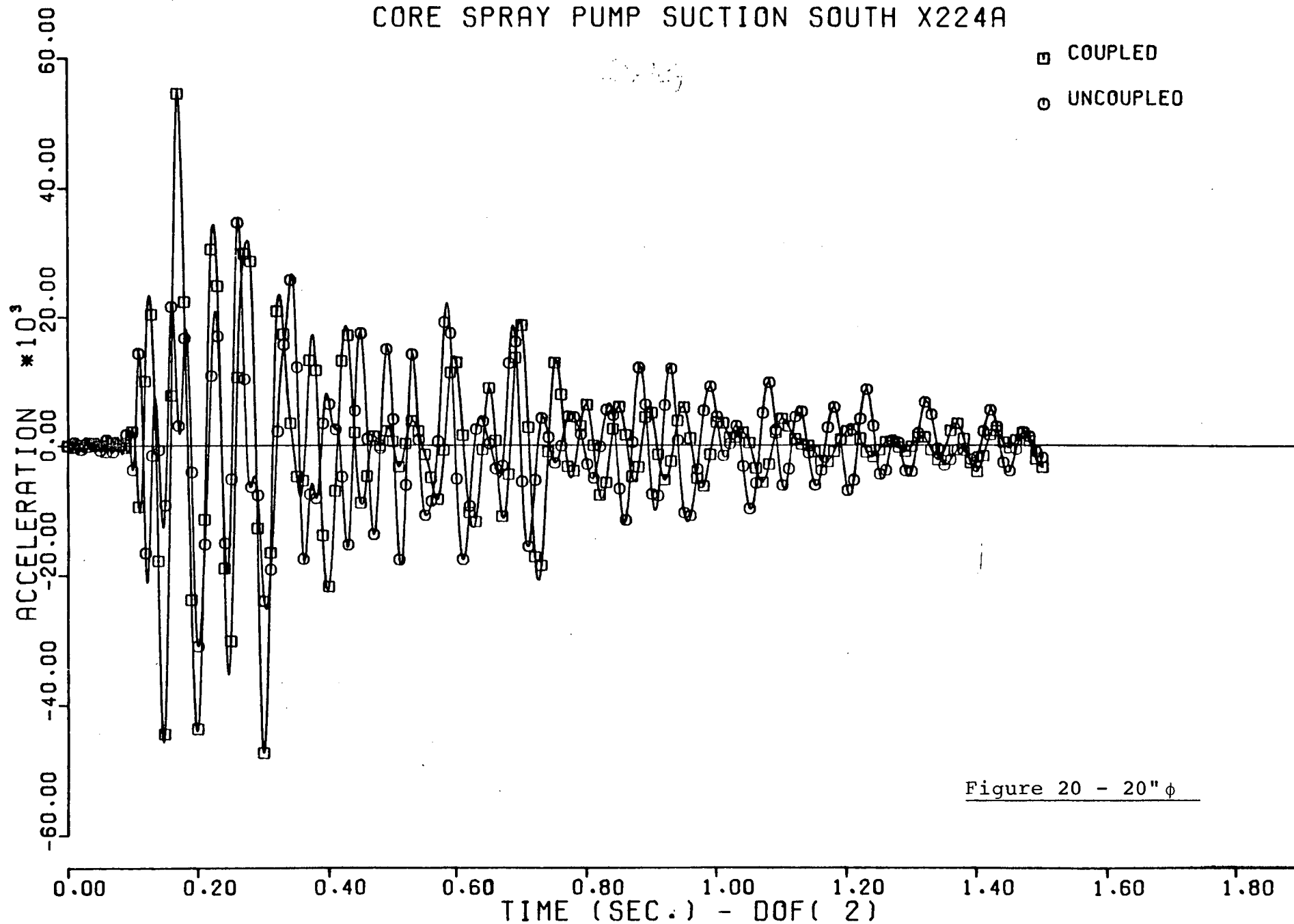


Figure 20 - 20"  $\phi$

CORE SPRAY PUMP SUCTION SOUTH X224A

276

- COUPLED
- UNCOUPLED

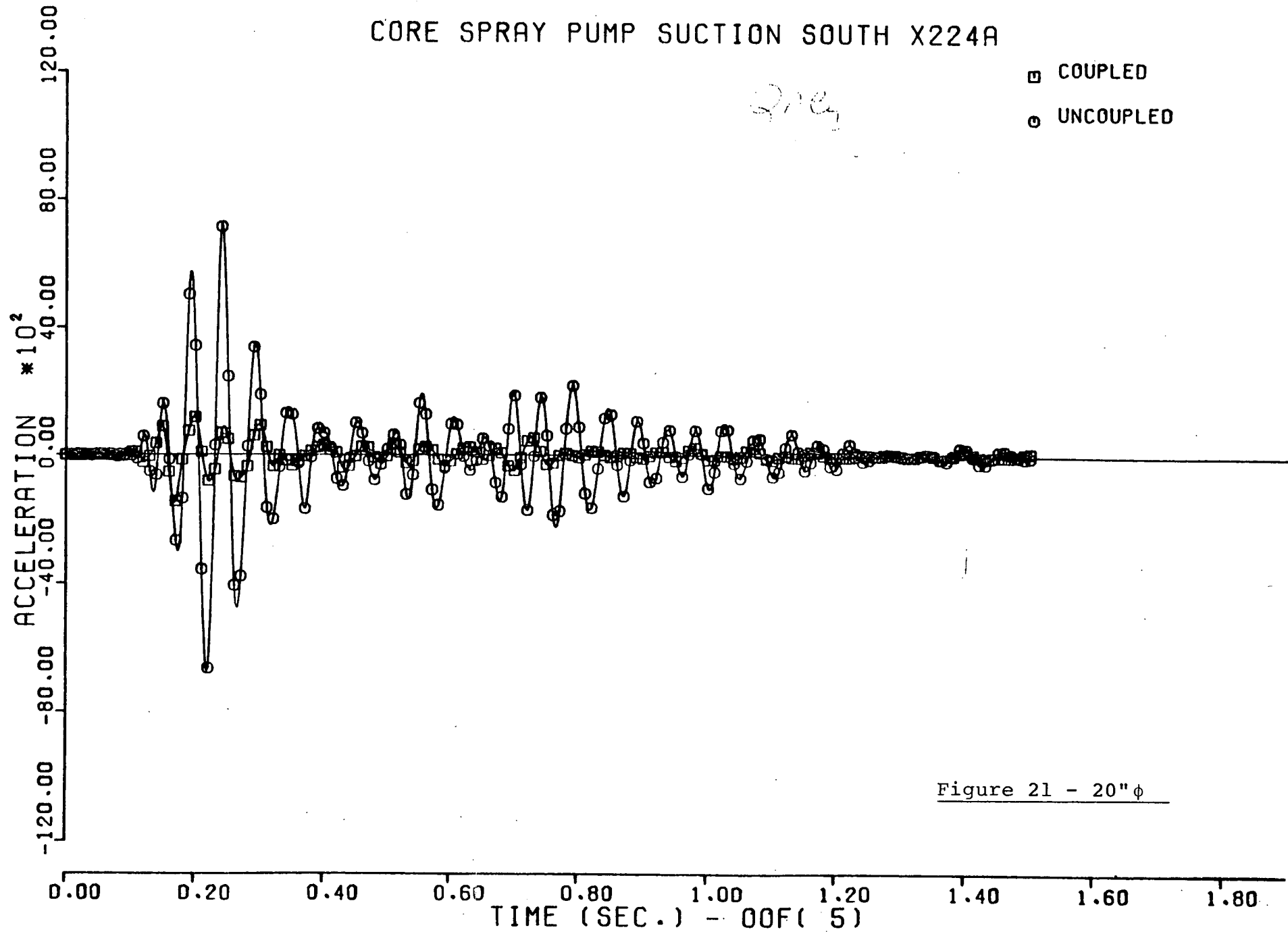


Figure 21 - 20" φ